Chaos, Solitons and Fractals 160 (2022) 112211

Contents lists available at ScienceDirect

Chaos, Solitons and Fractals

Nonlinear Science, and Nonequilibrium and Complex Phenomena

journal homepage: www.elsevier.com/locate/chaos

Hamilton energy, complex dynamical analysis and information patterns of a new memristive FitzHugh-Nagumo neural network

Zeric Tabekoueng Njitacke [a,b,c,*], Clovis Ntahkie Takembo [a], Jan Awrejcewicz [c], Henri Paul Ekobena Fouda [d], Jacques Kengne [b,e]

[a] Department of Electrical and Electronic Engineering, College of Technology (COT), University of Buea, P.O.Box 63, Buea, Cameroon
[b] Research Unit of Automation and Applied Computer (URAIA), Electrical Engineering Department of IUT-FV, University of Dschang, P.O. Box 134, Bandjoun, Cameroon
[c] Department of Automation, Biomechanics and Mechatronics, Lodz University of Technology, Lodz, Poland
[d] Laboratory of Mecanics, Department of Physics, Faculty of Science, University of Yaounde I, P.O. Box 812, Yaoundé, Cameroon
[e] Center for Nonlinear Systems, Chennai Institute of Technology, Chennai, Tamil Nadu, India

ARTICLE INFO

Article history:
Received 14 February 2022
Received in revised form 11 April 2022
Accepted 9 May 2022
Available online xxxx

Keywords:
FitzHugh-Nagumo neuron
Memristive autapse
Hamilton energy
Circuit implementation
Modulational instability
Information patterns

ABSTRACT

This paper presents and studies the dynamics of a single neuron, followed by the network of an improved FitzHugh-Nagumo model with memristive autapse. The investigation on the single neuron revealed that, for the set of the system parameters used for our study, the improved model experiences hidden dynamics. The Hamilton energy of the proposed model is established by exploiting the Helmholtz theorem. It is found that the external current has no effect on that energy and only the memristive autapse strength is able to affect the energy released by the considered neuron. The study of the dynamics of the proposed model revealed neuronal behaviors such as quiescent, bursting, spiking, and hysteretic dynamics characterized by the coexistence of firing patterns for the same set of parameters. The electronic circuit of the proposed model is constructed and simulated in the Pspice environment, and the obtained results match well with those obtained from the direct investigations of the mathematical model of the introduced neuron. Furthermore, a chain network of 500 identical neurons with memristive autapses is built and information pattern stability is investigated numerically via modulational instability under memristive autapse strength. It is found that with initial conditions taken as slightly modulated plane waves, the new network supports localized information patterns with traits of synchronization as a means of information coding. Also, by fixing the stimulation current, higher autaptic couplings resulted in new localized pattern formation, confirming the new information coding pattern and possible mode transition. This could provide a possible application in the building of artificial neurons.

1. Introduction

The nervous system is made up of an interconnection of a large number of neurons. A neuron is an essential unit in the brain structure since it plays some important functions such as the processing, transport, and storage of information. This is why, to study the complex dynamical behavior of the brain a large number of artificial neurons have been developed and investigated in the literature. Among these artificial neurons, are the Hopfield neural network model [1–4], the Hodgkin-Huxley neuron [5], the Chay model [6], the Izhikevich neuron [7], the FitzHugh-Nagumo (FN) model [8], the Morris-Lecar neuron [9], the 2-D Hindmarsh-Rose (HR), the 3-D-HR model [10,11], and the Rulkov model [12]. For example, in ref. [13], the authors investigated the dynamics of a single non-autonomous Hopfield neuron with a memristive self-synaptic connection. They showed that the introduced model was able to exhibit homogeneous extreme multistability. Of particular interest, they proposed a non-invasive control method that enables them to select any attractor among the coexisting ones. The phenomenon of broken symmetry in the solitary solutions of the Hodgkin-Huxley neuron model has been investigated in ref. [14]. In their work, the authors also showed the necessary and sufficient conditions for having bright and dark solitary solutions in that model. The phenomenon of the noise-delayed decay at the network level by considering scale-free neuronal networks and under the realistic assumption of noise being due to the stochastic nature of voltage-gated ion channels that are embedded in the neuronal membranes has been investigated in ref. [48]. In ref. [49], the spiking regularity of a single stochastic Hodgkin-Huxley neuron under the effects of ion channel blocking and autaptic connection has been investigated. The study of the authors revealed that the neuron was able to exhibit multiple coherence

* Corresponding author at: Department of Electrical and Electronic Engineering, College of Technology (COT), University of Buea, P.O. Box 63, Buea, Cameroon.
E-mail address: zerictabekoueng@yahoo.fr (Z.T. Njitacke).

https://doi.org/10.1016/j.chaos.2022.112211
0960-0779/

resonance behaviors induced by autaptic time delay at an appropriate level of ion channel blocking and autaptic coupling strength. Equally, the investigation of the cooperative effects of autapse and ion channel block on the collective firing regularity of Newman-Watts small-world networks of stochastic Hodgkin-Huxley neurons has been addressed in ref. [50].

The global dynamics of a Chay neuron has been investigated in ref. [15]. Using some common nonlinear analysis tools, the authors showed the occurrence of some neuronal behaviors such as bursting and spiking. More importantly, an FPGA implementation of their considered neuron model has been carried out to validate their theoretical analyses. In ref. [16], the authors investigated a model of the Fitzhugh-Nagumo neuron with memristive autapse. Their study revealed that the proposed model was able to exhibit extreme multistability. Their results have been finally validated with the circuit implementation of the considered model. The multistable dynamics of an autonomous Morris-Lecar neuron has been addressed in ref. [17]. During their study, diverse neuronal behaviors such as chaotic bursting, chaotic tonic-spiking, and periodic bursting behaviors were found. Also, the results were further validated based on a microcontroller development board. A model of a 4D memristive Hindmarsh-Rose has been investigated in ref. [18]. Using the Helmholtz theorem, the Hamilton energy of the proposed model was derived and used to characterize the variety of bifurcations and firing activities found in that model. Based on some of the quoted neuron models, the collective behavior of the neurons has been widely studied based on the interconnection of quoted artificial neurons through various types of artificial synapse. Chemical synapse [19], electrical synapse [20,21], hybrid synapse [22,23], Josephson junction synapse [24], and memristive synapse [25,26] are some of them. Among works devoted to the study of small-world networks of neurons, Zhou et al. [21] investigated the collective behavior of Hindmarsh-Rose neurons based on the Erdos-Rényi random network. Based on either excitatory chemical synapses or electrical synapses, slow-wave activity was generated.

In ref. [27], the authors considered a discretized version of the Izhikevich neuron model and found that electromagnetic flux can act as an order parameter in the sense that it can tune different firing patterns under the variation of electromagnetic flux. Hussain et al. [28] investigated the dynamics of a network of multi-weighted Fitzhugh-Nagumo neurons, taking into account the effect of electrical, chemical, and ephaptic couplings. The effects of those coupling types on the chimera states and complete synchronization exhibited by the networks were analyzed. When the temperature coefficient was varied, chimera states were able to occur in a network of thermosensitive Fitzhugh-Nagumo (FHN) neurons [29]. In ref. [30], authors investigated a Hindmarsh-Rose neuronal network. They found that the interconnected neurons were able to exhibit chimera states. Furthermore, they investigated the effect of noise and found that when the control parameter of the noise is increased, the chimera states are progressively suppressed. In ref. [31], various types of chimera states were found in a network of Hindmarsh-Rose neurons in the presence or absence of an electric field. In ref. [32], the authors investigated a network of 3D Hindmarsh-Rose neurons under the effect of an electrical autapse. Many scientists and engineers have employed diverse FHN neural networks in order to investigate cooperative behaviors such as wave propagation, synchronization, pattern formation, stochastic and coherent resonance, in excitable media under many physical factors such as noise, thermal fluctuation, electric field, time delays, electromagnetic induction and radiation. Zhang et al. [33] investigated memory effects via pattern formation and synchronization in chain FHN neurons with memristive synapse and found that when the synapse with memory is activated, the electrical activities of neurons are modulated to induce mode transition. Wu et al. [34] investigated complex electrical activities in cardiac tissue created by magnetic flux and found that spiral waves encounter breakup and turbulent electrical activities. The authors in ref. [35]constructed a discrete network of FHN neurons with autaptic synapse under electromagnetic radiation and found that under high intensity and frequency electromagnetic radiation, the propagating impulse waves encountered turbulent electrical activity, with patterns breakdown into a homogeneous state. Indeed, information coding pattern within the nervous system is closely linked to pattern formation and wave propagation within neural networks [36,37]. Recall that the memristor used as a synapse in some neuronal circuits is the fourth basic electronic component, besides the resistor, capacitor, and inductor. It has been used by Bao et al. [52] to investigate the effect of the threshold electromagnetic induction on the dynamics of a 2D Hindmarsh-Rose neuron model. In ref. [53], the coexistence of the firing activities has been investigated in two Morris-Lecar neurons coupled via a memristive synapse. Not only for biological models of neurons, memristive devices are also used to build Tabu learning neurons [54], which belong to the classes of neurons with adapting synapses. In this paper, we will construct a chain memristive FHN network and monitor information patterns stability via modulational instability as driven by autaptic coupling. The remaining part of this work is structured as follows: In Section 2, the mathematical model of the FHN neuron with memristive autapse is proposed. The Helmholtz theorem is used to calculate the Hamilton energy required for the occurrence of the firing pattern. In Section 3, numerical simulations are used to investigate the nonlinear phenomena exhibited by the introduced neuron model. Section 4 is devoted to the electronic circuit implementation of the newly introduced neuron model. In Section 5, the process of the information patterns in memristive autaptic FHN neural networks is explored. Lastly, in Section 6, we summarize the paper and present some perspectives for further research work.

2. Model description

2.1. Design of the FHN neuron with memristive autapse

Based on the definition of the memristor [38], a voltage-controlled generic model is designed as it can be observed on its state-dependent Ohm's law followed by its state equation given by:

$$\begin{cases} i = G(w)v = \alpha \sin(w)v \\ \dfrac{dw}{dt} = g(w,v) = \cos(w) + v \end{cases} \tag{1}$$

Based on memristor equations above, the model of FHN neuron with memristive autapse is given as:

$$\begin{cases} \dot{x} = x - bx^3 - y + i - \alpha \sin(w)x \\ \dot{y} = \dfrac{1}{\varepsilon}(x + a - cy) \\ \dot{w} = \cos(w) + x \end{cases} \tag{2}$$

In Eq. (2), x is the potential of the membrane of the FHN neuron also called fast variable, y is the retrieval or recovery variable related to the fast current of either Na^+ or K^+. w stands for the inner variable of the memristive autapse. $cos(w) + x$ represents the superposition of the magnetic flux leakage and the membrane potential enabling variation on magnet flux. $\alpha \sin(w)$ stands for memductance and $\alpha \sin(w)x$ the memristive autapse current. It shows the modulation of time varying field on the gap junction of the membrane. i represents an external forcing current while α represents the memristive autapse strength. In many upgraded memristor-based excitable systems, many researchers have examined wave propagation via pattern generation [35,40]. Takembo et al. [35] stated that by utilizing a controlled pitch of electromagnetic radiation, they were able to achieve flawless intercellular communication in a memristor-based neural network. Qian et al. [40] investigated the effects of network topology and other system characteristics on spatiotemporal dynamics in excitable homogeneous random networks in a systematic way. Further investigation of the pattern formation has to be done in this work using an improved

FHN neural network using the following positive parameters: $a = 0.7$, $b = 1/3$, $c = 0.8$, $\varepsilon = 13$, α and i are tuneable.

2.2. Energy released

The energy consumption of a neuron or coupled neurons is commonly associated with a Hamiltonian function in the field of neuroengineering. That function is generally based on the Helmholtz theorem-based mathematical model of the considered neuron. To achieve this goal, for a given neuronal system $\dot{x} = f(x)$, the vector field $f(x)$ is expressed as a sum of a conservative vector fields $f_c(x)$ and a dissipative vectors fields $f_d(x)$ as provided in Eq. (3):

$$f(x) = f_c(x) + f_d(x) \tag{3}$$

As a result, given the conservative component, the neuronal system's Hamilton energy should follow the following rule:

$$\nabla H^T f_c = 0 \tag{4}$$

The dissipation of the energy due to $f_d(x)$ should satisfy the equation

$$\nabla H^T f_d = \dot{H} \tag{5}$$

The conservative and dissipative vector fields of the FHN neuron with memristive autapse under consideration are given as follows using the above-mentioned formula:

$$f_c = \begin{bmatrix} -y + i - \alpha w \\ \frac{1}{\varepsilon}(a + x) \\ x \end{bmatrix} \tag{6}$$

$$f_d = \begin{bmatrix} x - bx^3 - \alpha \sin(w)x + \alpha w \\ \frac{-c}{\varepsilon} y \\ \cos(w) \end{bmatrix} \tag{7}$$

As a result of Eq. (4), the Hamilton function must satisfy the condition.

$$(-y + i - \alpha w)\frac{\partial H}{\partial x} + \left(\frac{1}{\varepsilon}(a + x)\right)\frac{\partial H}{\partial y} + x\frac{\partial H}{\partial w} = 0 \tag{8}$$

The consistent energy function that fulfills both Eqs. (4) and (5) is given by

$$H = (-y + i - \alpha w)^2 + \frac{1}{\varepsilon}(a + x)^2 + \alpha x^2 \tag{9}$$

In addition the derivative of that energy function is provided in Eq. (10)

$$\dot{H} = \dot{x}\left(\frac{2}{\varepsilon}(a + x) + 2\alpha x\right) + \dot{y}\,(-2(-y + i - \alpha w)) + \dot{w}\,(-2\alpha(-y + i - \alpha w)) \tag{10}$$

The average energy is obtained by defining the time average of the Hamilton energy function as,

$$h = \frac{1}{T}\int_{t_0}^{t_0+T} H(x, y, w)dt \tag{11}$$

And its derivative as

$$\dot{h} = \frac{1}{T}\int_{t_0}^{t_0+T} \dot{H}\,(x, y, w)dt \tag{12}$$

3. Dynamical behavior of the single FHN neuron

This section is devoted to the investigation of the dynamical behavior of the FHN with a memristive autapse. Two-parameter diagram based on energy, maximum Lyapunov exponent, and bifurcation diagram, are used to characterize the global behavior of the model. In addition, numerical simulations are performed using parameters and variables in extended precision mode with fixed step time of 5×10^{-3}. Fig. 1 shows the evolution of energy as well as its derivatives in the considered neurons.

Fig. 1 shows the evolution of energy as well as its derivatives in the considered neurons. For example, Fig. 1(a) is obtained when the external current and the memristive autapse strength are simultaneously varied. According to the diagram, the increase in external current has no effect on the neuron's energy. In contrast, when the memristive autapse strength increases, the energy exchanges of the considered model also increase. As such, that parameter will be very crucial in studying information pattern stability in a network of such neurons. Finally, Fig. 1(b) also highlights that the derivative of the energy of the neuron increases with the value of the memristive autapse strength.

When the previous two parameters of the considered model are again varied simultaneously and the maximum Lyapunov exponent is

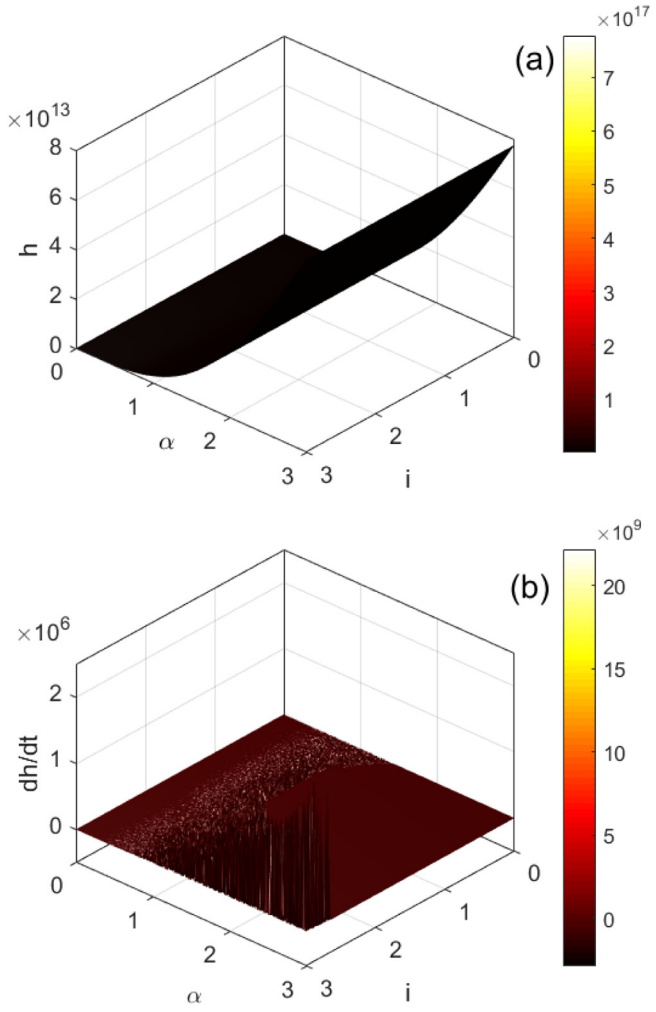

Fig. 1. Evolution of Hamilton energy of the introduced FHN neuron when two parameters are both varied in (a) with the corresponding derivative in (b). With initial conditions are (0.1,0,0). As it can be seen in these figures, the Hamilton energy of the model increases when the external current and the memristive autapse strength are simultaneously varied.

recorded at each iteration, the diagram in Fig. 2(a) with its enlargement in Fig. 2(b) is obtained. From the zoom of that two-parameter Lyapunov exponent diagram, three main behaviors are recorded. Stable behavior with rest patterns characterized by $\lambda_{max} < 0$, periodic behaviors with regular patterns are supported by $\lambda_{max} = 0$ while patterns with chaotic behaviors are supported $\lambda_{max} > 0$. As it can be seen in those two-parameter diagrams, there are several windows of switching between periodic and chaotic behaviors. For a discrete value of the external current $i = 0$, the bifurcation diagram of the Fig. 3(a) with its corresponding graph of the maximum Lyapunov exponent in Fig. 3 (b) have been computed by varying the memristive autapse strength α.

From these diagrams, two sets of data are found when increasing (black) and decreasing (magenta) the control parameter α. The model under consideration exhibit the period doubling bifurcation phenomenon as well as hysteretic dynamics characterized by the coexistence of bifurcations. The phase portrait of Fig. 4(a) and the corresponding time series of Fig. 4(b) show that chaotic busting is one of the behaviors experienced by the model.

For a discrete value $\alpha = 0.95$, the bifurcations diagrams of Fig. 5 (a) and (b) are obtained with the corresponding graph of the maximum Lyapunov exponent presented in Fig. 5(c). The hysteretic dynamics previously mentioned is equally found. That hysteretic dynamics is

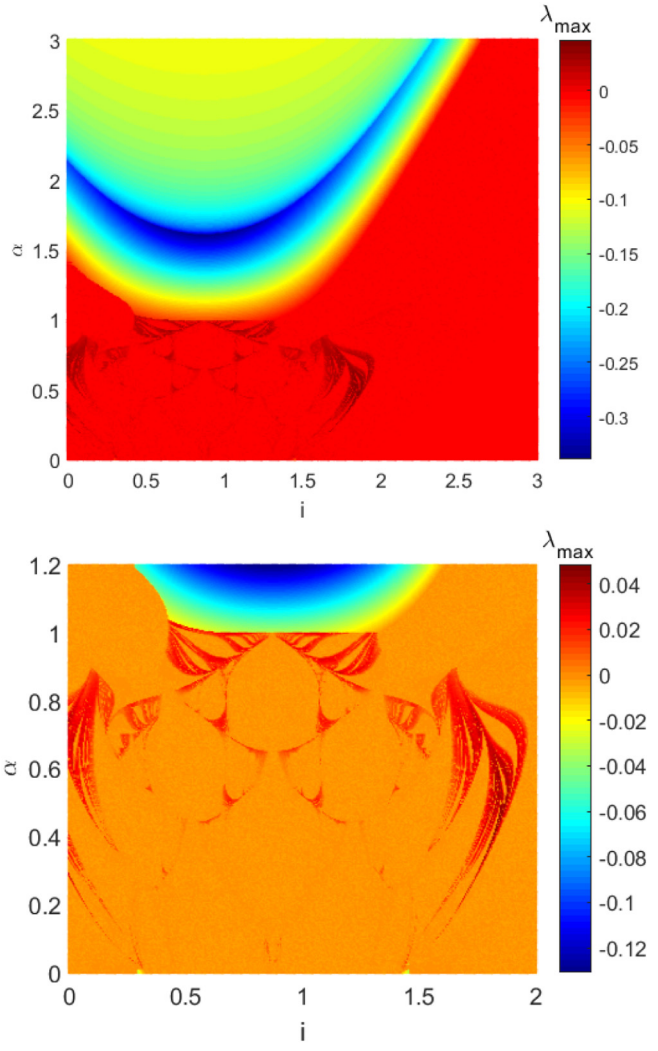

Fig. 2. Two-parameter Lyapunov exponent showing the global dynamics of the memristive neuron in (a) with the corresponding zoom in (b). With initial conditions are (0.1,0,0). From these figures, rest states are characterized by $\lambda_{max} < 0$, periodic states are characterized by $\lambda_{max} = 0$ while chaotic states are characterized by $\lambda_{max} > 0$.

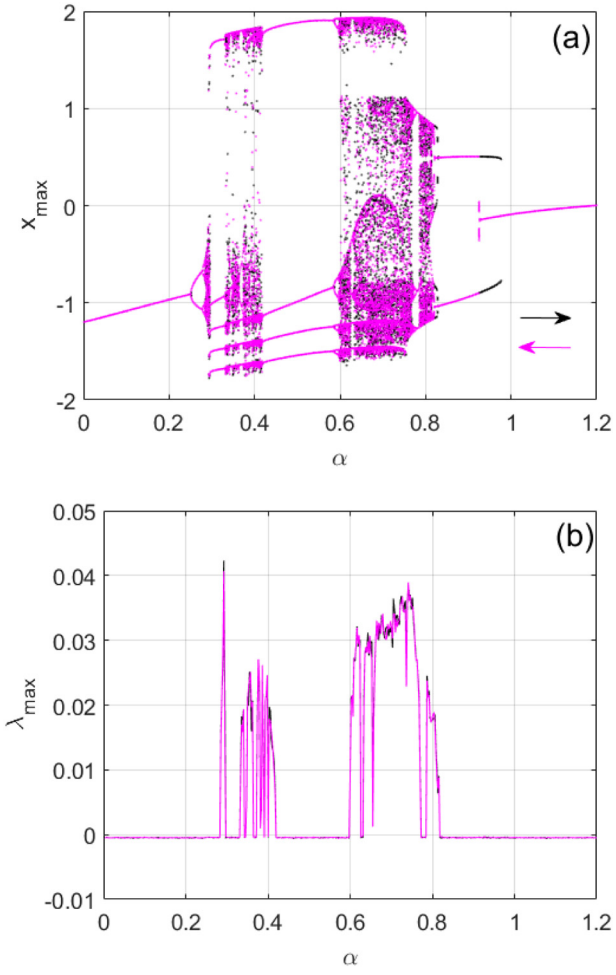

Fig. 3. Bifurcation diagram with the corresponding graph of the Largest Lyapunov exponent obtained by varying the memristive strength. They are obtained for $i = 0$ with initial conditions are (0.1,0,0). Using the graph of the maximum Lyapunov exponent as argument, periodic states are characterized by $\lambda_{max} = 0$ while chaotic states are characterized by $\lambda_{max} > 0$.

supported by the coexistence of three firing activities. One chaotic spiking behavior and two periodic spiking behaviors were observed, as evident by the superimposed phase portraits of Fig. 6(a) and their corresponding time series of Fig. 6(b). The effect of the initial conditions on the energy released by the proposed neuron model during the coexistence of patterns. As it can be seen in Fig. 6(c) and (d), the average value of the Hamilton energy of the chaotic patterns is $h \leq 135$ and the one with periodic patterns is $h > 135$. Therefore it is trivial the basin of attraction of the coexisting chaotic patterns is greater than the one of the coexisting periodic patterns. The equilibrium point of the considered model are obtained by solving the set of equations $\dot{x}=\dot{y}=\dot{w}=0$. After computing the equilibrium points using the software Maple 18, for some discrete values that give Figs. 4 and 6, we discover that there exist no real solutions to the equilibrium points of Eq. (2). So the FHN neuron with memristive autapse under consideration has no equilibrium points for those set of parameter. Therefore, it exhibits hidden electrical activities.

4. Circuit implementation

In this section, our main objective is to further support the obtained results from the previous investigations by using a circuit designed for the proposed FHN neuron with memristive autapse. The circuit has been realized as it can be seen on Fig. 7 in the Pspice simulation

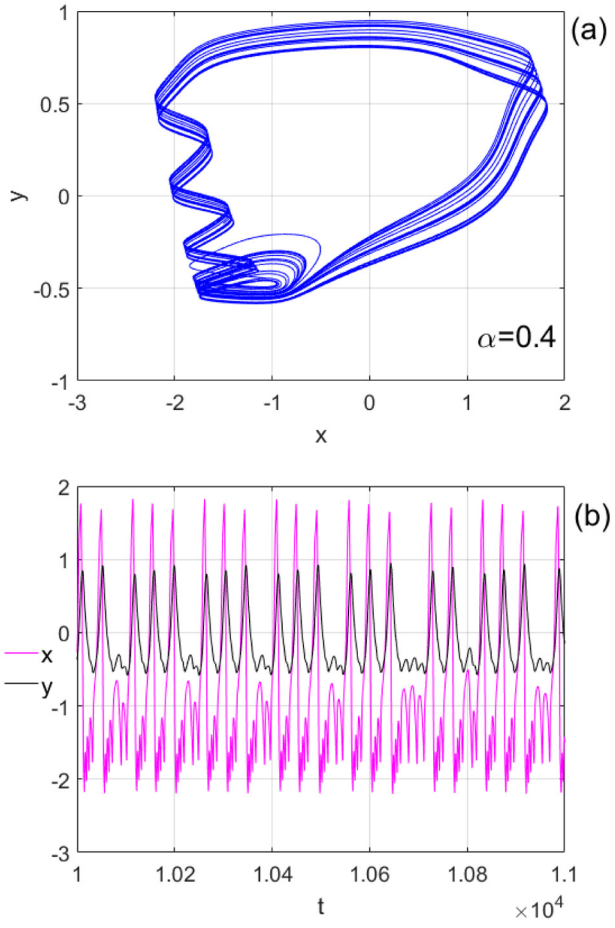

Fig. 4. (a) Phase portrait with the corresponding time series supporting chaotic bursting exhibited by the considered model with initial conditions (0.1,0,0). From the time series, the membrane potential x of the neuron appears as the fast variable while the retrieval variable y appears as the slow variable.

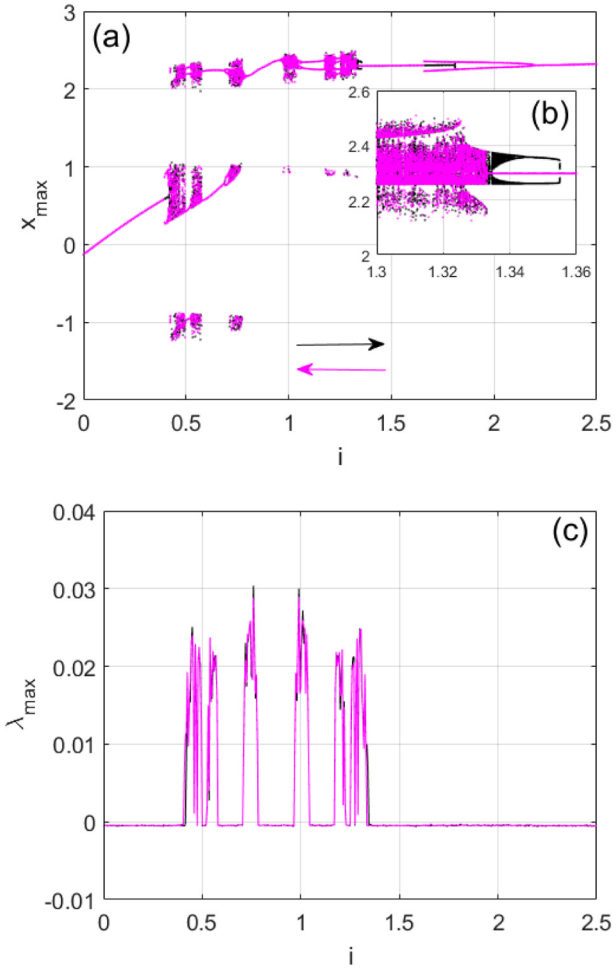

Fig. 5. (a) Bifurcation diagram with the corresponding zoom (b) showing the evolution of the behavior of the considered neuron. (c) is the largest Lyapunov exponent associated to (a). these diagrams are obtained for $\alpha = 0.95$ with initial condition (0.1,0,0). Using the graph of the maximum Lyapunov exponent as argument, periodic states are characterized by $\lambda_{max} = 0$ while chaotic states are characterized by $\lambda_{max} > 0$.

environment using operational amplifiers *TL*084, resistors, capacitors, DC and AC voltage source, DC power supply $\pm 15V$ symmetric, analog multipliers realizable with *AD*633*JN*, trigonometric function blocks realizable with *AD*639*AD*. For more details, the trigonometric function converter *AD*639*AD* can be used to implement the sine or cosine circuit module in physical terms, which was reported in ref. [51]. In contrast, the PSpice model of trigonometric function is just an ideal component that doesn't require any power supply. On Fig. 7, the main FHN circuit is made of two integrators, one inverter and two multipliers, while the main circuit of the memristive autapse is made of one integrator, one inverter two trigonometric blocks and one multiplier. Since the maximal amplitude of the phase error is greater than the supply voltage of the circuit, it is good to resize that state variable (inner variable of the memristive autapse) within the voltage range supportable by operational amplifiers. to avoid saturation. So considering $w^{'} = w/1000$, the mathematical model of the coupled neurons from Kirchhoff's electrical circuit law is given as in Eq. (13).

$$\begin{cases} C_1\dfrac{dX}{dt} = \dfrac{1}{R_3}X - \dfrac{1}{R_{b1}}X^3 - \dfrac{1}{R_1}Y + \dfrac{1}{R_4}V_5 - \\ \dfrac{1}{R_\alpha}\sin(1000W')X \\ C_2\dfrac{dY}{dt} = \dfrac{1}{R_e}X - \dfrac{1}{R_{c1}}Y + \dfrac{1}{R_{a1}}V_2 \\ C_3\dfrac{dW'}{dt} = \dfrac{1}{R_{21}}\cos(1000W') + \dfrac{1}{R_{20}}X \end{cases} \tag{13}$$

Considering $t = \tau RC, V_0 = 1V, x = \frac{X}{V_0}, y = \frac{Y}{V_0}, w' = \frac{W'}{V_0}$ and comparing Eq. (13) with Eq. (2) the value of the parameters of the circuit are given as: $R_{b_1} = \frac{R}{b_1} = 30k\Omega, V_2 = \frac{a_2 R_{a_1}}{\varepsilon R} = 0.0538V, R_{c_1} = \frac{\varepsilon R}{c_1} = 162.5k\Omega, R_e = \varepsilon R = 130k\Omega, R_{20} = 1000R, R_{21} = 1000R, V_5 = \frac{R_4}{R} i = tuneable, R_\alpha = \frac{R}{\alpha} = tuneable$. For $C = 10nF$ and all other resistor $R_i = R = 10k\Omega$ the investigation of the circuit of the memristive FHN circuit is investigated in Pspice environment.

Fig. 8 shows the time series of the chaotic bursting exhibited by the model in (a), the 2D projection of the attractors is provided in (b) as well as the corresponding frequency spectra in (c). The good accord is observed between them and those obtain from the numerical investigations. In the same line, Fig. 9 shows the coexistence different stable states from circuit of the memristive FHN neuron. Those coexisting attractors match well with their numerical equivalent of Fig. 6(a). Therefore, the accordance between these approaches further supports the fact that the results obtained in this work were not related to an artifact.

5. Information patterns of a new memristive FHN neural networks

The network version of the introduced model in this work used to study information patterns is given as

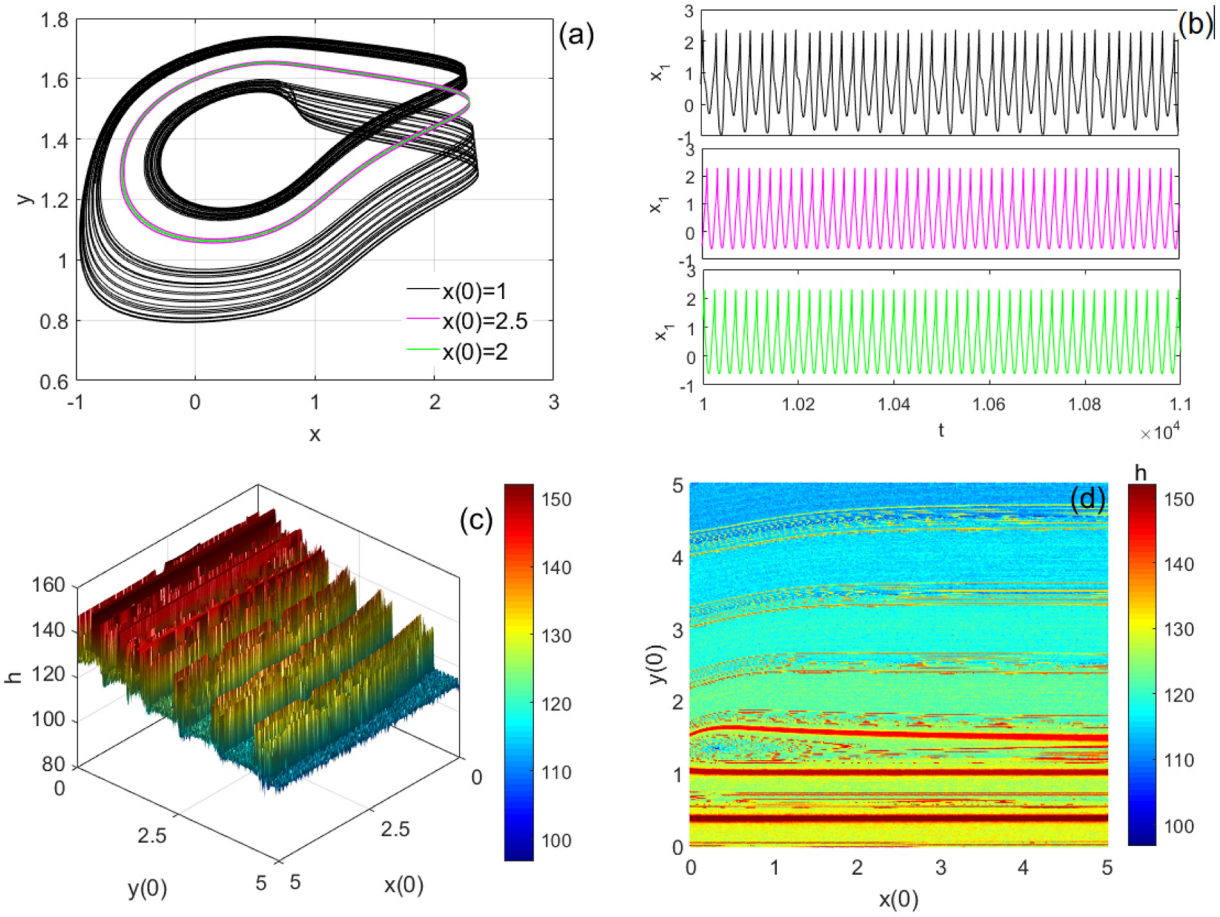

Fig. 6. (a) Phase portraits with the corresponding time series showing coexistence of three electrical activities for $i = 1.336$ with initial condition (1,0,0) for black, (2.5,0,0) for magenta and (2,0,0) for green. The related energy to each coexisting attractor is provided in (c) and (d). (For interpretation of the references to colour in this figure legend, the reader is referred to the web version of this article.)

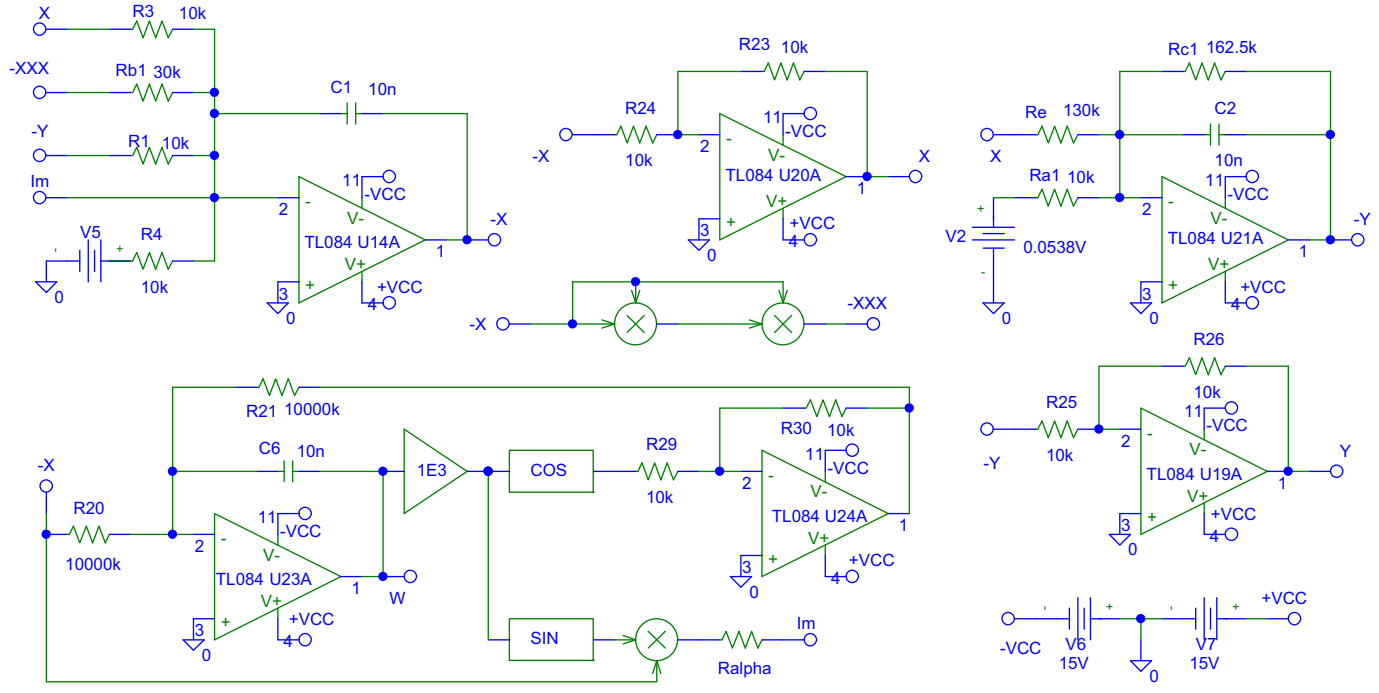

Fig. 7. The Circuit implementation of the introduced neuron model with memristive autapse. The circuit is made up of up to three intagrators, three inverters, and some special blocks made of multipliers, trigonometric functions, voltage sources, as well as a power supply $\pm 15v$ symmetric.

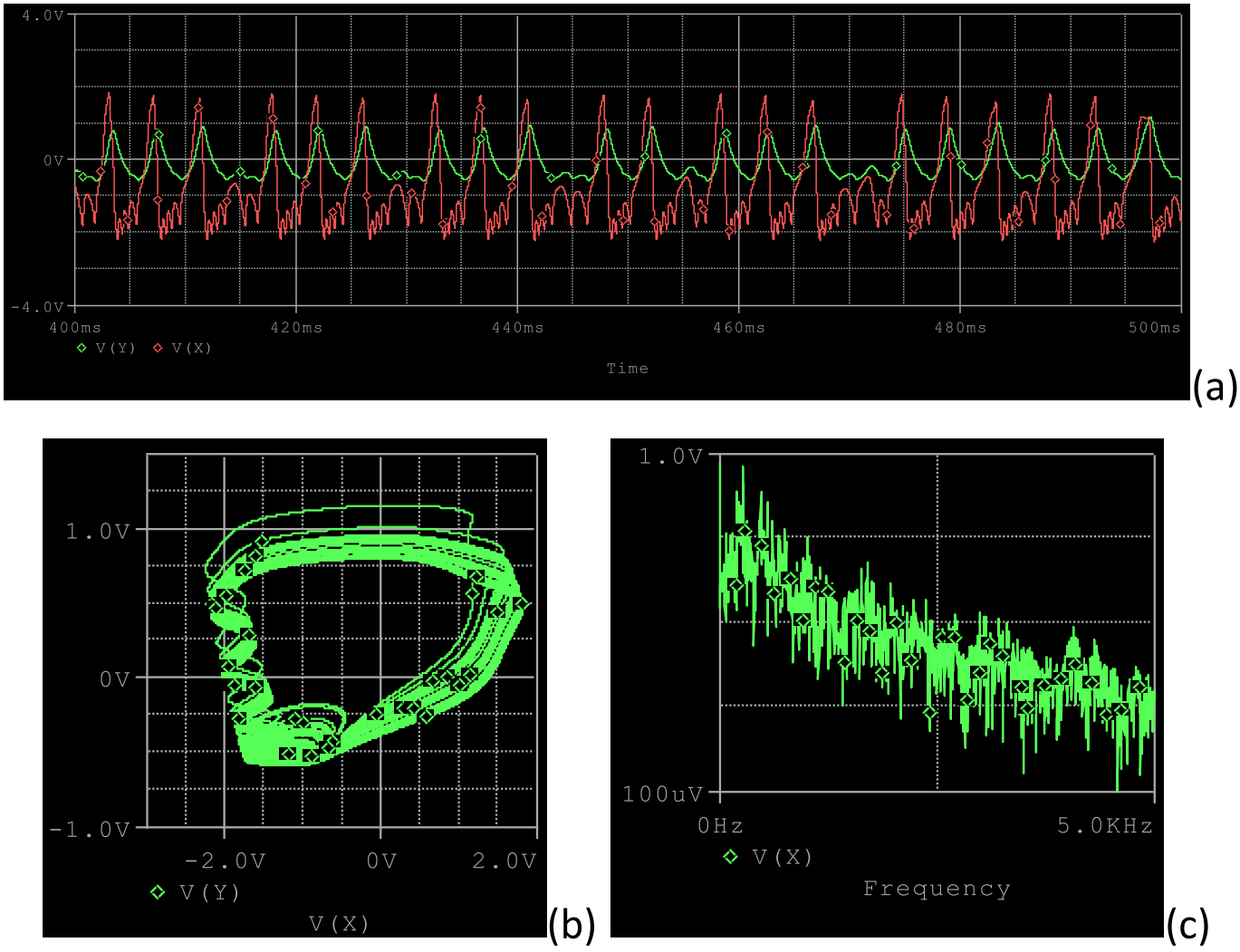

Fig. 8. Pspice simulation showing bursting oscillation of the considered neuron obtained for $R_\alpha = 25k\Omega$, $V_5 = 0V$ with initial conditions $(0.01V, 0.1V, 0V)$.

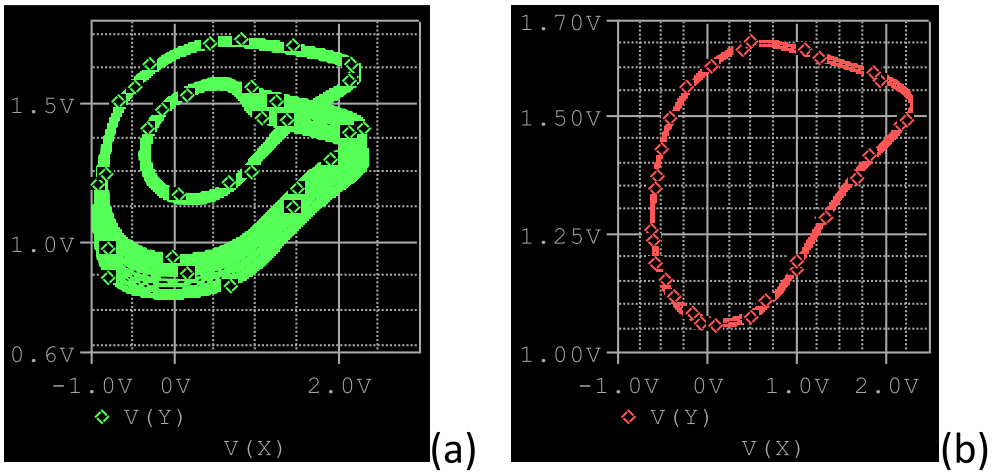

Fig. 9. Pspice simulation showing some coexisting attractors exhibited by the considered neuron, obtained for $R_\alpha = 10.526k\Omega$, $V_5 = 1.336V$ with initial conditions $(1V, 0V, 0V)$ for the chaotic attractor and $(2V, 0V, 0V)$ for the periodic attractor.

$$\begin{cases} \dfrac{dx_n}{dt} = x_n - bx_n^3 - y_n + i - \alpha \sin(w_n)x_n + \\ K(x_{n+1} - 2x_n + x_{n-1}) \\ \varepsilon \dfrac{dy_n}{dt} = x_n + a - cy_n \\ \dfrac{dw_n}{dt} = \cos(w_n) + x_n \end{cases} \tag{14}$$

where x_n is the transmembrane potential of neuron at the lattice site n, coupled to two nearest neighbors at the site $n-1$ and $n+1$, each with the coupling strength K. Indeed, we have considered a chain network of 500 identical neurons in our numerical simulations, in order to study the hidden spatiotemporal pattern of information in the form of wave propagation in the network under the memristor coupling (α). From early observations, the Hamiltonian energy of a neuron is increased as the memristor coupling is increased. This coupling parameter will undoubtedly affects instability/stability of information patterns within the network and thus constitute our motivation. In the process, we make use of modulational instability (MI) as a mechanism of wave pattern formation in nonlinear media. As a recall, MI is a well documented mechanism to predict modulated wave formation in physical systems [39,41,42]. MI is known to be a nonlinear-induced phenomenon, reported in many physical media, where small noise-driven amplitude and phase grow exponentially, due to the concomitant effects of dispersion and nonlinearity. The direct consequence is the breakup of any waveform (usually plane waves) into trains of modulated patterns. Here, we apply MI numerically in order to portray and discuss the effect of the new memristor coupling on pattern formation and hopefully believe these considerations open new routes in theoretical neurodynamics. In the numerical simulation, the set of Eq. (14) is integrated with the use of the fourth-order Runge-Kutta computational scheme having periodic boundary conditions. The network under consideration has 500 active nodes. Each of the initial conditions are slightly modulated plane waves with respective amplitudes of (1,0,0). Firstly, we maintain the simulation current (i) at zero and by selecting suitable values of memristor coupling (α), we present the 3D spatiotemporal pattern of membrane potential in Figs. 10, 11, 12.

From Fig. 10, we observe that for a memristor coupling $\alpha = 0.30$, the network of 500 identical neurons supports a breathing localized wave pattern in space and time. In other to evaluate the impact of α on the resulting patterns, we select higher values and results presented in Figs. 11 and 12. By selecting $\alpha = 0.40$ and $\alpha = 0.80$ in Figs. 11, 12 respectively, the network presents different dynamical motifs as the values of α are changed. This confirms our analytical predictions whereby the memristive autaptic coupling parameter has confirmed its ability in influencing the pattern of information within the network lattice. Extensive numerical simulations show that the intensity of the stimulation current (i) when varied has no influence on the information pattern within the network, which further confirms early prediction via the Hamiltonian energy of the system. This indicates the ability of our network to discriminate against environmental intensity current stimulation. It equally confirms the possible application of the presented network in building artificial neurons with such behaviors. Indeed, the various panels of localized wave patterns in Figs. 10, 11, 12 corresponds to spatially broadened pulses, or front waves, that are ubiquitous in excitable media like neurons and cell membranes [36,37,43,44]. In heart, for example, they have the responsibility to trigger harmonized contractions, whose failure can lead to important physiological disturbances

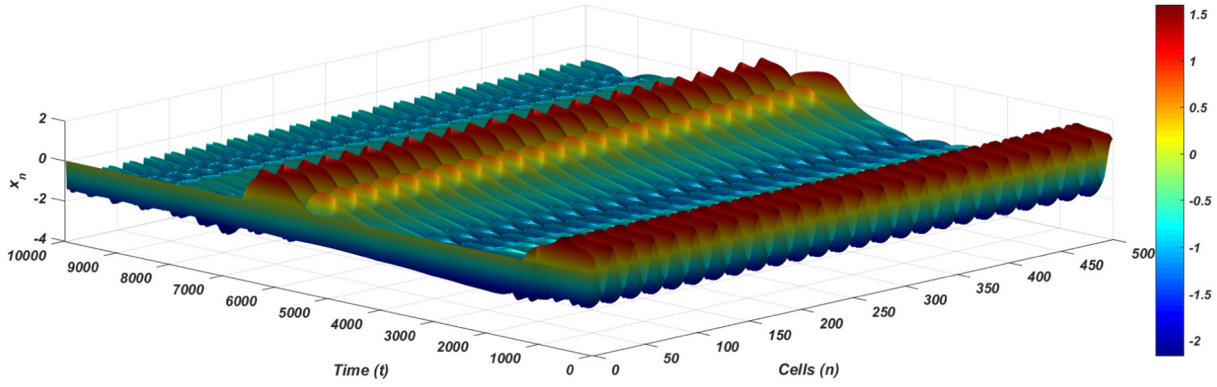

Fig. 10. 3D spatiotemporal pattern of membrane action potential, x_n calculated for the memristor coupling, $\alpha = 0.30$ and in the absent of the simulation current ($i = 0$), where $K = 0.05$.

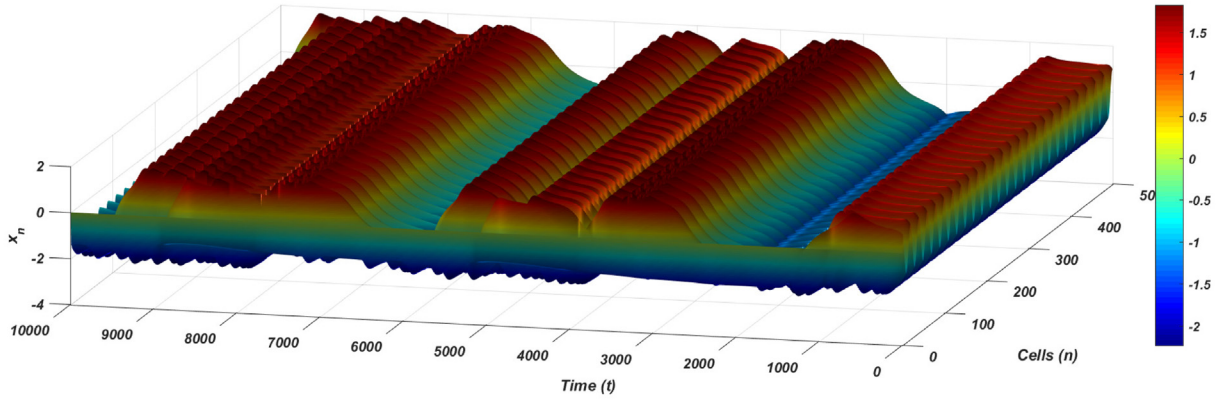

Fig. 11. 3D spatiotemporal pattern of membrane action potential, x_n calculated for the memristor coupling, $\alpha = 0.40$ and in the absent of the simulation current ($i = 0$), where $K = 0.05$.

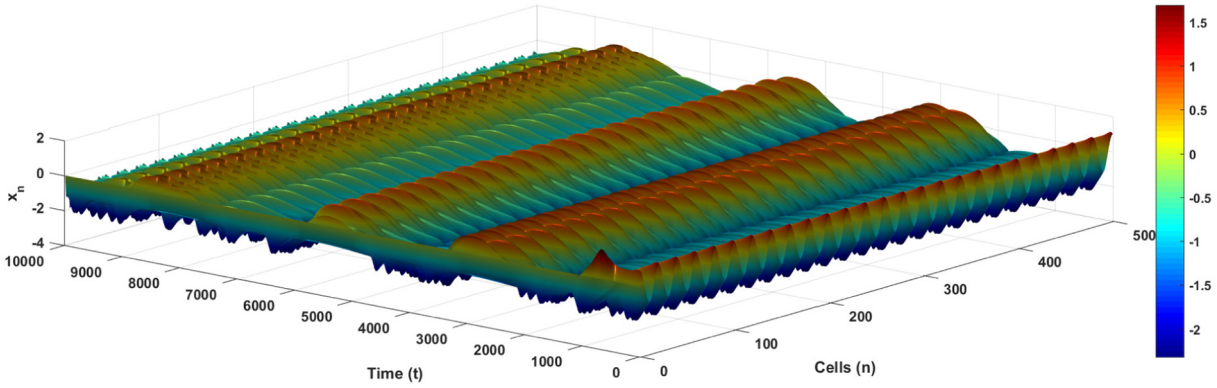

Fig. 12. 3D spatiotemporal pattern of membrane action potential, x_n calculated for the memristor coupling, $\alpha = 0.80$ and in the absent of the simulation current ($i = 0$), where $K = 0.05$.

[45–47]. From the physical theory of modulational instability, the memristive coupling increases the nonlinearity of the system under studies and consequently promotes the formation of modulated waves, whose formation are based on the concomitant effect of dispersion and nonlinearity in the media. From neuroscience perspective, our memristive network confirms its ability to support information processing and transmission in the form of modulated wave without an excitation current. This works provides a possible way of using the memristive autaptic current to influence information coding pattern within the nervous system. This could be a key factor in developing a stable artificial neural network. Finally from neurocomputational point of view, we earlier noticed an increase in the memristive autaptical coupling increases the total energy of the system. This increased in the energy of the system is closely linked to the stability of information pattern within the network. Through MI, we have confirmed this prediction by presenting the influence of the autaptic coupling on information coding pattern in the network. From the presentation, we sufficiently observe the information pattern and stability are closely linked to the autapses coupling.

6. Conclusion

In this contribution, a novel FitzHugh-Nagumo (FHN) neuron model with memristive autapse has been introduced; both the single and network of that neuron have been investigated. The study of the single neuron has revealed its hidden dynamics since it is equilibrium-free. Using the well-known Helmholtz formula, the Hamilton energy of the proposed neuron has been established. Among the control parameters that were the external current and the memristive autapse strength, only the second one was able to affect the energy released by the proposed neuron model. Using the two-parameter Lyapunov exponent and time series as an argument, the studies of the model revealed behaviors such as quiescent, bursting, spiking, and multistability. Of particular interest, an electronic circuit of the proposed neuron has been built and investigated to support the result of the theoretical investigation. Finally, the network of the proposed neuron has been built and information pattern stability has been investigated numerically via modulational instability under autaptic coupling parameter. It has been found that, the new network was able to support localized information patterns with traits of synchronization as a means of information coding.

CRediT authorship contribution statement

Zeric Tabekoueng Njitacke: Supervision, Investigation, Formal analysis, Writing – original draft, Writing – review & editing. **Clovis Ntahkie Takembo:** Writing – original draft, Investigation, Writing – review & editing. **Jan Awrejcewicz:** Supervision, Resources, Validation, Writing – review & editing. **Henri Paul Ekobena Fouda:** Validation, Writing – review & editing. **Jacques Kengne:** Supervision, Validation, Writing – review & editing.

Declaration of competing interest

The authors declare that they have no known competing financial interests or personal relationships that could have appeared to influence the work reported in this paper.

Acknowledgments

This work is partially funded by the Polish National Science Center under the Grant OPUS 14 No: 2017/27/B/ST8/01330.

References

[1] Njitacke ZT, Isaac SD, Nestor T, Kengne J. Window of multistability and its control in a simple 3D hopfield neural network: application to biomedical image encryption. Neural Comput & Applic. 2020:1–20.
[2] Njitacke ZT, Kengne J, Fotsin H. Coexistence of multiple stable states and bursting oscillations in a 4D hopfield neural network. Circuits Systems Signal Process. 2020;39:3424–44.
[3] Doubla Isaac S, Njitacke ZT, Kengne J. Effects of low and high neuron activation gradients on the dynamics of a simple 3D hopfield neural network. Int J Bifurcation Chaos. 2020;30:2050159.
[4] Tabekoueng Njitacke Z, Laura Matze C, Fouodji Tsotsop M, Kengne J. Remerging feigenbaum trees, coexisting behaviors and bursting oscillations in a novel 3D generalized hopfield neural network. Neural Process Lett. 2020:1–23.
[5] Hodgkin AL, Huxley AF. A quantitative description of membrane current and its application to conduction and excitation in nerve. J Physiol. 1952;117:500–44.
[6] Chay TR. Chaos in a three-variable model of an excitable cell. Physica D. 1985;16:233–42.
[7] Izhikevich EM. Simple model of spiking neurons. IEEE Trans Neural Netw. 2003;14:1569–72.
[8] Izhikevich EM, FitzHugh R. Fitzhugh-nagumo model. Scholarpedia. 2006;1:1349.
[9] Tsumoto K, Kitajima H, Yoshinaga T, Aihara K, Kawakami H. Bifurcations in Morris? Lecar neuron model. Neurocomputing. 2006;69:293–316.
[10] Hindmarsh J, Rose R. A model of the nerve impulse using two first-order differential equations. Nature. 1982;296:162–4.
[11] Hindmarsh JL, Rose R. A model of neuronal bursting using three coupled first order differential equations. Proc R Soc London, Ser B. 1984;221:87–102.
[12] Xu Q, Liu T, Feng C-T, Bao H, Wu H-G, Bao B-C. Continuous non-autonomous memristive rulkov model with extreme multistability. Chin Phys B. 2021;30(12):128702.
[13] Doubla IS, Ramakrishnan B, Njitacke ZT, Kengne J, Rajagopal K. Hidden extreme multistability and its control with selection of a desired attractor in a non-autonomous hopfield neuron. AEU Int J Electron Commun. 2022;144:154059.
[14] Telksnys T, Navickas Z, Timofejeva I, Marcinkevicius R, Ragulskis M. Symmetry breaking in solitary solutions to the hodgkin-Huxley model. Nonlinear Dyn. 2019;97:571–82.
[15] Xu Q, Tan X, Zhu D, Bao H, Hu Y, Bao B. Bifurcations to bursting and spiking in the Chay neuron and their validation in a digital circuit. Chaos, Solitons Fractals. 2020;141:110353.
[16] Li Z, Guo Z, Wang M, Ma M. Firing activities induced by memristive autapse in Fitzhugh-nagumo neuron with time delay. AEU Int J Electron Commun. 2021;142:153995.

[17] Bao B, Yang Q, Zhu L, Bao H, Xu Q, Yu Y, Chen M. Chaotic bursting dynamics and coexisting multistable firing patterns in 3D autonomous Morris?Lecar model and microcontroller-based validations. Int J Bifurcation Chaos. 2019;29:1950134.
[18] Xu L, Qi G, Ma J. Modeling of memristor-based hindmarsh-rose neuron and its dynamical analyses using energy method. Appl Math Model. 2022;101:503–16.
[19] Burić N, Todorović K, Vasović N. Synchronization of bursting neurons with delayed chemical synapses. Phys Rev E. 2008;78:036211.
[20] Shaffer A, Harris AL, Follmann R, Rosa Jr E. Bifurcation transitions in gap-junction-coupled neurons. Phys Rev E. 2016;94:042301.
[21] Zhou J-F, Jiang E-H, Xu B-L, Xu K, Zhou C, Yuan W-J. Synaptic changes modulate spontaneous transitions between tonic and bursting neural activities in coupled Hindmarsh-Rose neurons. Phys Rev E. 2021;104:054407.
[22] Liu Z, Wang C, Zhang G, Zhang Y. Synchronization between neural circuits connected by hybrid synapse. Int J Mod Phys B. 2019;33:1950170.
[23] Yao Z, Zhou P, Zhu Z, Ma J. Phase synchronization between a light-dependent neuron and a thermosensitive neuron. Neurocomputing. 2021;423:518–34.
[24] Zhang Y, ChunNi W, Jun T, Jun M, GuoDong R. Phase coupling synchronization of FHN neurons connected by a josephson junction. Sci China Technol Sci. 2020;63:2328–38.
[25] Li Y. Simulation of memristive synapses and neuromorphic computing on a quantum computer. Phys Rev Res. 2021;3:023146.
[26] Zhang G, Guo D, Wu F, Ma J. Memristive autapse involving magnetic coupling and excitatory autapse enhance firing. Neurocomputing. 2020;379:296–304.
[27] Muni SShankar, Rajagopal K, Karthikeyan A, Arun S. Discrete hybrid Izhikevich neuron model: nodal and network behaviours considering electromagnetic flux coupling. arXiv e-prints; 2021. arXiv: 2105.10415.
[28] Hussain I, Jafari S, Perc M, Ghosh D. Chimera states in a multi-weighted neuronal network. Phys Lett A. 2022;424:127847.
[29] Hussain I, Jafari S, Ghosh D, Perc M. Synchronization and chimeras in a network of photosensitive FitzHugh?Nagumo neurons. Nonlinear Dyn. 2021:1–11.
[30] Wang Z, Xu Y, Li Y, Kapitaniak T, Kurths J. Chimera states in coupled hindmarsh-rose neurons with -stable noise. Chaos, Solitons Fractals. 2021;148:110976.
[31] Simo GR, Njougouo T, Aristides R, Louodop P, Tchitnga R, Cerdeira HA. Chimera states in a neuronal network under the action of an electric field. Phys Rev E. 2021;103:062304.
[32] Aghababaei S, Balaraman S, Rajagopal K, Parastesh F, Panahi S, Jafari S. Effects of autapse on the chimera state in a hindmarsh-rose neuronal network. Chaos, Solitons Fractals. 2021;153:111498.
[33] Zhang G, Wang C, Alzahrani F, Wu F, An X. Investigation of dynamical behaviors of neurons driven by memristive synapse. Chaos, Solitons Fractals. 2018;108:15–24.
[34] Wu F, Wang C, Xu Y, Ma J. Model of electrical activity in cardiac tissue under electromagnetic induction. Sci Rep. 2016;6:28.
[35] Takembo CN, Mvogo A, Ekobena Fouda HP, Kofané TC. Effect of electromagnetic radiation on the dynamics of spatiotemporal patterns in memristor-based neuronal network. Nonlinear Dyn. 2019;95:1067–78.
[36] Takembo CN, Nyifeh P, Fouda HE, Kofane T. Modulated wave pattern stability in chain neural networks under high-low frequency magnetic radiation. Physica A. 2022:126891.
[37] Takembo CN. Information pattern stability in memristive Izhikevich neural networks. Mod Phys Lett B. 2022;36(12):2250021. https://doi.org/10.1142/S021798492250021X.
[38] Leon C. Everything you wish to know about memristors but are afraid to ask. Radioengineering. 2015;24:319.
[39] Tagne ATankou, Takembo C, Ben-Bolie H, Ateba POwona. Localized nonlinear excitations in diffusive memristor-based neuronal networks. PLOS ONE. 2019;14:e0214989.
[40] Qian Y, Liu F, Yang K, Zhang G, Yao C, Ma J. Spatiotemporal dynamics in excitable homogeneous random networks composed of periodically self-sustained oscillation. Sci Rep. 2017;7:1–13.
[41] Takembo CN, Fouda HPE. Effect of temperature fluctuation on the localized pattern of action potential in cardiac tissue. Sci Rep. 2020;10:1–12.
[42] Panguetna CS, Tabi CB, Kofané TC. Low relativistic effects on the modulational instability of rogue waves in electronegative plasmas. J Theor Appl Phys. 2019;13:237–49.
[43] Kivshar YS, Peyrard M. Modulational instability in discrete lattices. Phys Rev A. 1992;46:3198.
[44] Tankou AS, Takembo CN, Ben-Bolie GH, Ateba POwona. Localized nonlinear excitations in diffusive memristor-based neuronal network. PLoS ONE. 2019;14(6):e0214989.
[45] Takembo CN, Ekobena HP. Effect of temperature fluctuation on the localized pattern of action potential in cardiac tissue. Sci Rep. 2020;10(1):15087.
[46] Tabi CB, Maina I, Ekobena HP, et al. Discrete impulses in coupled nerve fibres. Chaos. 2015;25:043118.
[47] Mvogo A, Takembo CN, Ekobena HP, Kofane TC. Pattern formation in diffusive excitable systems under magnetic flow effects. Phys Lett A. 2017;381:2264–71.
[48] Uzuntarla M, Uzun R, Yilmaz E, Ozer M, Perc M. Noise-delayed decay in the response of a scale-free neuronal network. Chaos, Solitons Fractals. 2013;56:202–8.
[49] Uzun R. Influences of autapse and channel blockage on multiple coherence resonance in a single neuron. Appl Math Comput. 2017;315:203–10.
[50] Uzun R, Yilmaz E, Ozer M. Effects of autapse and ion channel block on the collective firing activity of Newman?Watts small-world neuronal networks. Physica A. 2017;486:386–96.
[51] Chen M, Ren X, Wu H, Xu Q, Bao B. Interpreting initial offset boosting via reconstitution in integral domain. Chaos, Solitons Fractals. 2020;131:109544.
[52] Bao H, Hu A, Liu W, Bao B. Hidden bursting firings and bifurcation mechanisms in memristive neuron model with threshold electromagnetic induction. IEEE Trans Neural Netw Learn Syst. 2019;31:502–11.
[53] Bao B, Yang Q, Zhu D, Zhang Y, Xu Q, Chen M. Initial-induced coexisting and synchronous firing activities in memristor synapse-coupled Morris?Lecar bi-neuron network. Nonlinear Dyn. 2020;99:2339–54.
[54] Bao B, Zhu Y, Ma J, Bao H, Wu H, Chen M. Memristive neuron model with an adapting synapse and its hardware experiments. Sci China Technol Sci. 2021;64:1107–17.